JOURNAL OF MOLECULAR SPECTROSCOPY **101**, 71–82 (1983)

Variationally Exact Ro-vibrational Levels of the Floppy CH_2^+ Molecule

JONATHAN TENNYSON

SERC Daresbury Laboratory, Daresbury, Nr. Warrington WA4 4AD, United Kingdom

AND

BRIAN T. SUTCLIFFE

Department of Chemistry, University of York, Heslington, York YO1 5DD, United Kingdom

Ro-vibrational calculations are performed on the CH_2^+ radical using a method recently developed for atom–diatom systems. The vibrational fundamentals obtained are 2998.8, 718.3, and 3270.7 cm^{-1}, in good agreement with recent results. Band origins for several higher vibrational levels are also obtained. Calculations with $J = 1$ show that the Coriolis interaction play a significant role and two alternative embeddings are discussed. Use of correlation parameters confirms that CH_2^+ belongs to no idealized class of molecules in keeping with its "floppy" nature.

1. INTRODUCTION

Recently, Bartholomae, Martin, and Sutcliffe (BMS) (*1*), and Carter and Handy (HC) (*2*) calculated vibrational band origins for the $^2A_1$ ground state of the CH_2^+ radical. This molecule is of special interest because of the floppiness of H–C–H bending coordinate. In particular the $D_{\infty h}$ linear saddle point lies only 931 cm^{-1} above the equilibrium C_{2v} structure (*2*).

Both works used the Whitehead–Handy method (*3*) to solve forms of the Eckart Hamiltonian (*4*) due to Watson (*5, 6*) and encountered difficulties with Watson's Hamiltonian for nonlinear molecules (*5*). This was attributed to the finite amplitude of the vibrations in the singular (linear) domain of this Hamiltonian. BMS circumvented this problem by weighting their basis so as to suppress any vibrational amplitude in the linear region. This approach will be faulty if it does not allow the sampling of a physically significant region of the potential (*7*).

HC used Watson's Hamiltonian for linear molecules (*6*) to solve the CH_2^+ problem. This approach is formally correct, as it avoids singularities in the physically important region of the Hamiltonian, but involves expanding the wavefunction as displacements from a pseudo-equilibrium linear structure. This led to convergence and numerical difficulties which prevented HC from obtaining satisfactory results for more than the band origins (*8*). The experience of these two calculations suggests that any approach based on the concept of an equilibrium structure will show similar difficulties for floppy molecules such as CH_2^+. We cite, for example, the shifts in average geometry shown by both KCN and LiCN with vibrational excitation (*9, 10*).

0022-2852/83 $3.00

Recently we have developed a variational method for dealing with the bound states of floppy (large amplitude) atom–diatom systems using a close-coupling approach (*11*) and have generalized it to provide a method for the full triatomic problem (*12, 13*). In this paper we show how this method can be adapted to describe A_2B systems for which the linear A–B–A structure is important, and use it to obtain the energies of the low-lying ro-vibrational states for CH_2^+. For this we use the potential fitted by HC in the form of Sorbie and Murrell (*14*) to the ab initio results of BMS. This means that our results can be compared directly to those obtained using the more conventional approach to the ro-vibrational problem.

2. METHOD

It was shown in Ref. (*11*) that if a triatomic molecule was considered as an atom $\{1\}$ colliding with a diatomic system $\{2\text{–}3\}$ then the Hamiltonian for internal motion could be written in terms of the space-fixed coordinates $\mathbf{t}_i$, with

$$\mathbf{t}_1 = \mathbf{x}_1 - \mathbf{x}_d$$

$$\mathbf{t}_2 = \mathbf{x}_3 - \mathbf{x}_2 \tag{1}$$

as

$$\hat{H}^t = -\frac{\hbar^2}{2\mu}\nabla^2(\mathbf{t}_1) - \frac{\hbar^2}{2\mu_d}\nabla^2(\mathbf{t}_2) + \mathbf{V}. \tag{2}$$

In these equations the x_i represent the lab. fixed coordinates of the nuclei with

$$\mathbf{x}_d = (m_2 + m_3)^{-1}(m_2\mathbf{x}_2 + m_3\mathbf{x}_3) \tag{3}$$

and

$$\mu^{-1} = m_1^{-1} + (m_2 + m_3)^{-1}$$

$$\mu_d^{-1} = m_2^{-1} + m_3^{-1}. \tag{4}$$

In Ref. (*11*) a body-fixed coordinate system was introduced by means of an orthogonal matrix $\mathbf{C}$ such that

$$\mathbf{t}_i = \mathbf{C}\mathbf{z}_i \tag{5}$$

with $\mathbf{C}$ defined by choosing

$$\mathbf{z}_1 = \begin{pmatrix} 0 \\ 0 \\ R \end{pmatrix}, \qquad \mathbf{z}_2 = r\begin{pmatrix} \sin\theta \\ 0 \\ \cos\theta \end{pmatrix}, \tag{6}$$

where R is the length of $\mathbf{t}_1$, r the length $\mathbf{t}_2$, and θ the angle between $\mathbf{t}_1$ and $\mathbf{t}_2$. This choice corresponds to choosing a coordinate system in which the z axis is along $\mathbf{t}_1$ with θ in the range $(0, \pi)$, the diatom lies in the positive half of the $(x$–$z)$ plane.

It is, however, possible to follow Istomin *et al.* (*15*) and choose an embedding such that

$$\mathbf{z}_1 = R\begin{pmatrix} \sin\theta \\ 0 \\ \cos\theta \end{pmatrix}, \qquad \mathbf{z}_2 = \begin{pmatrix} 0 \\ 0 \\ r \end{pmatrix}, \tag{7}$$

which is such that the z axis is along the diatomic part (t_2) and the atom (t_1) lies in the positive half of the (x–z) plane. Figure 1 illustrates the embedded coordinate system.

With either embedding the Hamiltonian is of the form

$$\hat{H} = \hat{K}_{VR} + \hat{K}_V + V(R, r, \theta) \tag{8}$$

where

$$\hat{K}_V = -\frac{\hbar^2}{2\mu}\frac{1}{R^2}\frac{\partial}{\partial R}\left(R^2\frac{\partial}{\partial R}\right) - \frac{\hbar^2}{2\mu_d}\frac{1}{r^2}\frac{\partial}{\partial r}\left(r^2\frac{\partial}{\partial r}\right) - \frac{\hbar^2}{2}\left(\frac{1}{\mu R^2} + \frac{1}{\mu_d r^2}\right)\frac{1}{\sin\theta}\frac{\partial}{\partial\theta}\left(\sin\theta\frac{\partial}{\partial\theta}\right) \tag{9}$$

$$\hat{K}_{VR} = \frac{1}{2}\left(\frac{1}{\mu_1 v_1^2}(\Pi_x^2 + \Pi_y^2) + \left(\frac{\cot^2\theta}{\mu_1 v_1^2} + \frac{\operatorname{cosec}^2\theta}{\mu_2 v_2^2}\right)\Pi_z^2\right) + \frac{\cot\theta}{2\mu_1 v_1^2}(\Pi_x\Pi_z + \Pi_z\Pi_x) + \frac{\hbar}{i}\frac{1}{\mu_1 v_1^2}\left(\frac{\partial}{\partial\theta} + \frac{\cot\theta}{2}\right)\Pi_y. \tag{10}$$

In Eq. (10) with the embedding of Eq. (6) $\mu_1 = \mu$, $v_1 = R$; $\mu_2 = \mu_d$, $v_2 = r$ and with the embedding of Eq. (7), $\mu_1 = \mu_d$, $v_1 = r$; $\mu_2 = \mu$, $v_2 = R$. In both embeddings the Jacobian for the volume element of integration is $R^2r^2 \sin\theta$. The Π_α are the components of the total angular momentum and, as explained in Ref. (*11*), are chosen to satisfy the normal commutation relations. They are functions of the Euler angles α, β, γ only. With the embedding of Eq. (6) these operators represent the angular momentum of the diatomic part about the atom–diatomic axis, while with the embedding of Eq. (7) they represent the angular momentum of the atom about the diatomic part.

As usual in a planar system, the sense of the third axis (in this case the y axis) is not determined by the embedding procedure but is chosen, once the other two axes have been determined, to form a right-handed system. In the present case this means that the two embedded coordinate systems differ from one another not just by a positive rotation about the y axis, but by an improper rotation in which the sense of the x axis changes as well. This means that associated Legendre polynomials $\Theta_{lq}(\theta)$

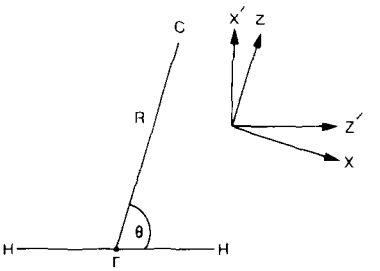

FIG. 1. Coordinate system: (x, z) are the axes for the embedding of Eq. (6) and (x', z') for that of Eq. (7).

(*16*) have a slightly different significance in each embedding in that $\Theta_{lq}(\theta)$ in one embedding is equivalent to $\Theta_{l-q}(\theta)$ in the other.

In either embedding, suitable angular functions are of the form

$$2^{1/2}[\Theta_{lq}(\theta)D^J_{Mq}(\alpha, \beta, \gamma) + (-1)^p\Theta_{l-q}(\theta)D^J_{M-q}(\alpha, \beta, \gamma)] \qquad p = 0, 1; \quad q > 0$$

$$\Theta_{l0}(\theta)D^J_{M0}(\alpha, \beta, \gamma) \qquad p = 0; \qquad q = 0 \tag{11}$$

where D^J_{Mq} is a rotation matrix in the convention of Brink and Satchler (*17*). J, the total angular momentum, and $J + p$, the parity, are good quantum numbers. Following convention (*18*), we label $p = 0$ states e and $p = 1$ states f. For the embedding of Eq. (6), $q = k$, the projection of J along **R**, and for embedding of Eq. (7), $q = \Omega$, the projection of J along **r**.

If $\hat{H}$ is allowed to operate from the right on the functions (11) and the result multiplied from the left by their complex conjugate, integrating over all angular coordinates gives an effective Hamiltonian which operates only on the radial coordinates.

$$\hat{H}' = \hat{K}'_{VR} + \hat{K}'_V + \delta_{qq'}\langle\theta_{l'q'}|V|\Theta_{lq}\rangle_{\theta,\alpha,\beta,\gamma} \tag{12}$$

$$\hat{K}'_V = \delta_{qq'}\delta_{ll'}\left[\frac{-\hbar^2}{2\mu R^2}\frac{\partial}{\partial R}\left(R^2\frac{\partial}{\partial R}\right) - \frac{\hbar^2}{2\mu_d r^2}\frac{\partial}{\partial r}\left(r^2\frac{\partial}{\partial r}\right) + \frac{\hbar^2}{2}l(l+1)\left(\frac{1}{\mu R^2} + \frac{1}{\mu_d r^2}\right)\right] \tag{13}$$

$$\hat{K}'_{VR} = \delta_{ll'}\frac{\hbar^2}{2\mu_1 v_1^2}[\delta_{qq'}\{J(J+1) - 2q^2\} - (1 + \delta_{q0})^{1/2}C^+_{Jq}C^+_{lq}\delta_{q',q+1}$$

$$- (1 + \delta_{q'0})^{1/2}C^-_{Jq}C^-_{lq}\delta_{q',q-1}] \tag{14}$$

where the significance of μ_1 and v_1 is as explained above and where

$$C^{\pm}_{nq} = [(n+1) - q(q+1)]^{1/2}. \tag{15}$$

The secular equations generated by Eq. (12) are the well-known close-coupled equations (*19*). These equations are diagonal in q, save for the off-diagonal Coriolis terms in $\hat{K}'_{VR}$. It is therefore computationally convenient, as explained in Ref. (*11*), if these terms can be neglected. Although the results of a calculation using Eq. (12) completely will be indifferent to the embedding chosen, this will not be the case if the off-diagonal Coriolis terms are neglected, and different results can be expected depending on the embedding. This matter is investigated later.

In this work, as previously (*11–13*), we follow Le Roy and Van Kranendonk (*20*) and use radial basis functions so the problem becomes one of diagonalizing a secular matrix. The acronym LC-RAMP (linear combination of radial and angular momentum product functions) has been coined for this variationally exact approach (*21*). As in Ref. (*12*), we write the radial basis functions

$$r^{-1}H_n(r)R^{-1}H_m(R). \tag{16}$$

Previously (*11–13*) we have used Morse-like functions for both these radial stretching coordinates. These are still appropriate for the H–H stretch:

$$H_n(y) = \beta^{1/2} N_{n\alpha} \exp(-y/2) y^{(\alpha+1)/2} L_n^{\alpha}(y) \tag{17}$$

$$y = A \exp[-\beta(r - r_e)] \tag{18}$$

where $N_{n\alpha}L_n^{\alpha}$ is a normalized Laguerre polynomial (*22*) and r_e the equilibrium value of r, A and β can be related to the dissociation energy D_e and fundamental vibrational frequency ω_e of the appropriate (pseudo) diatomic Morse curve

$$A = \frac{4D_e}{\omega_e}, \qquad \beta = \omega_e \left(\frac{\mu_d}{2D_e}\right)^{1/2} \tag{19}$$

and α is the integer closest to A. In practice r_e, D_e, and ω_e are optimized to give the best basis set expansion for each problem. As in Ref. (*12*), the integration over r was performed using a mixture of analytic integration (*23*) and Gauss–Laguerre quadrature (*24*).

As observed by ter Haar (*25*), the functions (17) do not obey the correct boundary conditions at $r = 0$ and can only be used if the wavefunctions have effectively vanished at this limit. This condition is satisfied by r for all triatomics, but not by R for CH_2^+ which has vibrational wavefunctions with finite amplitude for the linear H–C–H ($R = 0$) structure.

For the R coordinate spherical oscillator-like functions are thus appropriate:

$$H_m(R) = N_{m\eta}(\zeta R^2)^{(\eta+1)/2} \exp(-\zeta R^2/2) L_m^{\eta+1/2}(\zeta R^2) \tag{20}$$

where ζ equals $(\mu\omega)^{1/2}$ with ω equal to the fundamental R stretching frequency. For spherical oscillators $\eta = l$ (see Eq. (11)). However, this coupling of radial and angular functions is inconvenient to work with. We thus chose to work with η and ω as parameters which can be optimized for a particular problem; this gives an orthonormal basis complete for all m.

For the spherical oscillator-like basis functions the kinetic energy and moment of inertia matrix elements can be calculated analytically,

$$\left\langle H_{m'} \middle| \frac{-\hbar^2}{2\mu R^2} \frac{\partial}{\partial R}\left(R^2 \frac{\partial}{\partial R}\right) \middle| H_m \right\rangle$$

$$= N_{m'\eta} N_{m\eta} \frac{\hbar^2}{4\mu} \zeta^{1/2} \left[\delta_{m',m-1} \frac{\Gamma(m' + \eta + 3/2)}{m'!} + \delta_{mm'}(2m + \eta + 3/2) \right.$$

$$\left. \times \frac{\Gamma(m + \eta + 3/2)}{m!} - \eta(\eta + 1) \sum_{\sigma=0}^{m'} \frac{\Gamma(\sigma + \eta + 1/2)}{\sigma!} \right] \qquad m' \leqslant m \tag{21}$$

$$\left\langle H_{m'} \middle| \frac{\hbar^2}{2\mu R^2} \middle| H_m \right\rangle = N_{m'\eta} N_{m\eta} \frac{\hbar^2}{4\mu} \zeta^{1/2} \sum_{\sigma=0}^{\min(m',m)} \frac{\Gamma(\sigma + \eta + 1/2)}{\sigma!} \tag{22}$$

and the integral over the potential can be obtained using Gauss–Laguerre quadrature based on $L_M^{\eta+1/2}$ (*11, 24*).

To construct the effective radial motion operator of Eq. (12) the potential must be integrated over all the angular coordinates. This integral, which is the only one

coupling basis functions differing in l, is analytic if the potential is fitted as a Legendre expansion (*11*)

$$V(R, r, \theta) = \sum_{\lambda=0}^{\Lambda} V_\lambda(R, r) P_\lambda(\cos\theta). \tag{23}$$

However, not all triatomic potentials are conveniently represented in this form. We have thus generalized ATOMDIAT (*13*) to perform Gauss–Legendre quadrature (*24*) over a general potential, such as the CH_2^+ potential of Ref. (*2*). For each combination (r_i, R_j) required by the Gauss-Laguerre quadrature schemes in those coordinates we perform L point ($L = \Lambda + 2$) Gauss–Legendre quadrature to give an effective Legendre expansion at (r_i, R_j). Providing Λ is sufficiently large, this method entails no loss of accuracy over direct use of the potential. As in practice the radial matrix elements are formed before the integration over the angular coordinates (*12, 13*), this three-dimensional integration is performed outside the loop over angular basis functions and is thus computationally less expensive than the diagonalization of the secular matrix.

3. CALCULATIONS WITH $J = 0$

Table I shows the convergence of the Legendre expansion for the potential of Carter and Handy (HC) (*2*) for the equilibrium structure ($\theta = 90°$) and at a point a short distance from it. Clearly, the series is well converged for $\Lambda = 20$ and this value was used for all results presented here. Test dynamical calculations with $\Lambda > 20$ differed negligibly from ones with $\Lambda = 20$.

As a first step in performing the ro-vibrational calculations, it was necessary to select an optimized and saturated basis. For this purpose, we assumed that the three coordinates (R, r, θ) could be treated independently. For r, a basis set of 7 functions (all $n \leqslant 6$) with $r_e = 3.95a_0$, $D_e = 44\,000$ cm^{-1} and $\omega_e = 2630$ cm^{-1} saturated the basis so that adding a further function lowered the energy of the lowest five A_1 states

TABLE I

Convergence of the Legendre Expansion of Eq. (16) with Increasing Λ (Both geometries are for $r = 3.8541a_0$ and $R = 0.7539a_0$. Energies, in cm^{-1}, are relative to dissociated $C^+(^2P) + H(^2S) + H(^2S)$)

Λ	V/cm^{-1}	
	cos θ = 0	cos θ = 0.1
0	-53553.251	-53553.251
4	-73687.108	-73330.285
8	-74055.770	-73630.368
12	-74060.726	-73632.954
16	-74060.802	-73632.964
20	-74060.803	-73632.965
24	-74060.803	-73632.965

TABLE II

Band Origins (in cm^{-1}) for the $J = 0$ A_1 States, Relative to the Ground (0, 0, 0, 0, 0^e) State Energy of $-70\,400.619$ cm^{-1} (Vibrational assignments have been made where possible)

	Band Origin	$(J, v_1, v_2, v_3, \Omega^P)$
1	718.34	$(0,0,\ 2,0,0^e)$
2	1611.04	$(0,0,\ 4,0,0^e)$
3	2770.67	$(0,0,\ 6,0,0^e)$
4	2998.84	$(0,1,\ 0,0,0^e)$
5	3678.65	$(0,0,\ 8,0,0^e)$
6	4117.37	$(0,1,\ 2,0,0^e)$
7	4551.07	$(0,0,10,0,0^e)$
8	5598.47	
9	5702.34	
10	5881.92	

with $J = 0$ by less than 0.05 cm^{-1}. Inclusion of all angular functions with $l \leqslant 21$ gave similarly converged results. These convergence properties were found to hold equally for calculations on the $J = 0$ A_1 states (l = even) and $J = 0$ B_2 states (l odd).

For R, the same basis set is not optimal for all states. This is because all functions with $\eta = 0$ have amplitude at $R = 0$ whilst all functions with $\eta > 0$ do not. This means that the value of η selected as optimal depends on the nature of the state involved. We thus reoptimized η (and ω) for each set of quantum numbers. For the $J = 0$ A_1 states, nine functions (all $m \leqslant 8$) with $\eta = 0$ and $\omega = 13\,200$ cm^{-1} saturated the lowest five states to within 0.08 cm^{-1}. For the B_2 state $\eta = 0.95$ and $\omega = 17\,600$ cm^{-1} was found to be optimal. Tables II and III present our results for the $J = 0$ levels with A_1 and B_2 symmetry, respectively. The low-lying levels of both symmetry

TABLE III

Band Origins (in cm^{-1}) for the $J = 0$ B_2 States, Relative to the A_1 Ground (0, 0, 0, 0, 0^e) State (Vibrational assignments have been made where possible)

	Band Origin	$(J, v_1, v_2, v_3, \Omega^P)$
1	3270.60	$(0,0,0,1,0^e)$
2	3966.85	$(0,0,2,1,0^e)$
3	4839.45	$(0,0,4,1,0^e)$
4	5973.00	$(0,1,0,1,0^e)$
5	6772.28	
6	7287.78	

have been labeled using the conventional designations for a linear molecule (*26*). $(J, \nu_1, \nu_2, \nu_3, \Omega^P)$ where ν_1 is the symmetric stretch, ν_2 the bend, and ν_3 the asymmetric stretch. Although we would argue that it is strictly incorrect to regard CH_2^+ as a linear molecule, this labeling is convenient and still appropriate for the levels for which harmonic components can be assigned from the nodal structure of the vibrational modes. For the higher states, where the nodal structure is in general complicated, there is no simple way of classifying the vibrations (*9, 10*).

Table IV compares our fundamental frequencies and zero point energy with those calculated by BMS and HC. While our results confirm those of HC, BMS's band origins are clearly in error. This we ascribe to difficulties with Watson's Hamiltonian for nonlinear molecules (*5*) and the rather unusual functions used. Furthermore, it would seem that in the BMS calculations, the potential was sampled in regions that were not legitimately part of the domain of the Eckart Hamiltonian. This can happen in numerical integration if the Cartesian extrapolation of the normal coordinates causes points with $R < 0$ (or $\Theta > 180°$) to be sampled. If this occurs then the variational character of the result is destroyed. This phenomenon has also been remarked on by HC (*2, 8*). Conversely, it is encouraging to note that the saturated nature of our basis is reflected in a zero-point energy 2 cm^{-1} lower than HC obtained variationally for the same surface.

Unlike HC (*2, 8*), we have been able to converge several of the higher vibrational levels. In particular we note the rather unequal spacing between successive excitations of the ν_2 "bending" coordinate—which in our calculations is largely carried by the R basis. Such behavior has been observed in a one-dimensional calculation on CH_2 (*27*) and is characteristic of modes for which the lower states are localized in one part of a double minimum and higher states can cross the barrier. For CH_2^+, the barrier is only 931 cm^{-1} and when zero-point energy considerations are taken into account the $2\nu_2$ level must already be free to sample the linear region. Indeed, the zero-point energy of 3660 cm^{-1} is 5% less than that given by the harmonic formula $1/2(\nu_1 + 2\nu_2 + \nu_3) = 3853$ cm^{-1} and is a reflection of the anharmonicity (or floppiness) of CH_2^+ even in its lowest states.

4. ROTATIONALLY EXCITED STATES

For a full calculation with $J > 0$, the size of the secular problem grows rapidly unless it is possible to neglect the effect of the off-diagonal Coriolis terms. These

TABLE IV

Comparison of Fundamental Frequencies of the CH_2^+ Molecule and Ground State Energies (in cm^{-1})

Ref.	This work	BMS (1)	HC (2)
Ground state	-70400.619	-70519.6	-70398.669[a]
Zero point energy	3660.18	3541.2	3662.1
ν_1	2998.8	2935	2999
$2\nu_2$	718.3	908	718
ν_3	3270.7	3162	3271

[a] S. Carter, private communication

TABLE V

Calculation of the Lowest $J = 1^e$ Levels with and without the Off-Diagonal Coriolis Interactions, with Embeddings (6) and (7) (k and Ω are the projections of J along **R** and **r**, respectively)

z along R				z along r		
k	ℓ	No Coriolis	Full calculation	Ω	ℓ	No coriolis
1	odd	-70281.4	-70385.9	0	even	-70379.4
0	even	-70211.6	-70282.2	1	odd	-70281.4
1	even	-67009.6	-67112.5	0	odd	-67114.0
0	odd	-66956.2	-67012.0	1	even	-67009.6

terms have often been successfully neglected (*10, 11, 21*) and Table V compares the results of test calculations for $J = 1^e$ using the same basis (see Table VI below), for the complete Hamiltonian and with neglect of the off-diagonal Coriolis terms in both

TABLE VI

$J = 0$ and 1 States Calculated with $n \leqslant 5$, $m \leqslant 7$, $l \leqslant 17$ and Including All Coriolis Interactions ($J = 1$ energies in cm^{-1} are relative to the corresponding $J = 0$ term. Parity of l and Ω values are given for a calculation with the z axis along **r**. Vibrational assignments are given where possible)

J = 0			J = 1							
			ℓ odd				ℓ even			
ℓ even	ℓ odd	$\nu_1\nu_2\nu_3$	Ω	e	Ω	f	Ω	e	Ω	f
-70400.48		0 0 0	1	118.31			0	14.63	1	119.05
-69681.9		0 2 0	1	338.3			0	14.2	1	338.7
-69788.4		0 4 0	1	529.6			0	14.0	1	529.8
-67625.7		0 6 0	1	342.3			0	12.4	1	343.0
-67401.5		1 0 0	1	416.3			0	14.3	1	416.3
	-67129.0	0 0 1	0	16.5	1	119.4	1	117.0		
-66720.0		0 8 0	1	336.7			0	13.9	1	337.2
	-66431.4	0 2 1	0	18.3	1	340.4	1	335.2		
-66268.3		1 2 0	1	717.8			0	18.8	1	717.8
-65842.8		0 10 0	1	520.2			0	15.4	1	520.6
	-65554.7	0 4 1	0	23.7	1	532.0	1	522.4		
-64788.2			1	392.7			0	42.3	1	393.4
		η		0.95		0.0		0.0		0.95
		ω/cm^{-1}		17600		17600		17600		17600

embeddings. It should be noted that the parity of l changes between embedding as discussed in Section 2.

It is seen that k (the projection of J on the R axis) is a very poor quantum number. In particular the lowest $J = 1^e$ state is predicted to be 105 cm^{-1} too high if k is taken to be a good quantum number. This leads to a $J = 1^e \leftarrow 0$ transition frequency which is a factor of 7 too large. On the other hand Ω (the projection of J along the r axis) is quite a good quantum number giving the lowest $J = 1^e$ state only 6 cm^{-1} too high. This difference could have been anticipated as the expected value of R^{-2} is very much larger than the expected value of r^{-2}. Indeed R is zero for a linear structure. In discussing the results of the full calculations therefore, it would seem sensible to label according to Ω, rather than k, when identifying the various states. However, even in this embedding the off-diagonal Coriolis terms are too large to warrant their exclusion.

Table VI presents results for the $J = 1$ levels of CH_2^+ calculated with no approximations about the Coriolis terms. As a full $J = 1^e$ calculation was expensive with the full basis set of the last section, these results were calculated for a basis comprising all $n \leqslant 5$, $m \leqslant 7$, and $l \leqslant 17$ (432 functions for each $J = 0$ calculations). Results for the corresponding $J = 0$ calculation are also given. For the $J = 1^f$ calculations we reoptimized η and ω for the R basis set; for the $J = 1^e$ calculation of a full optimization proved too expensive and the results presented are the best ones from a few trial runs. In each case the values of η and ω actually used are shown. We notice that the rotational spacing with increasing vibrational excitation is far from uniform, indicating the importance of ro-vibrational mixing in this system.

HC obtained 15, 117, and 118 cm^{-1} for their best $J = 1 \leftarrow 0$ transition frequencies for the vibrational ground state (*2*). As these results were obtained using a truncated basis which overestimated the vibrational fundamentals by about 20 cm^{-1}, they agree surprisingly well with our values of 14.6, 118.3, and 119.1 cm^{-1}.

It is interesting to ask whether one should regard CH_2^+ as linear, bent, or a free rotor. To this end Yamada and Winnewisser (*28*) defined a correlation parameter which we can generalize as

$$\gamma^{YW}_{\nu_1\nu_2\nu_3} = 1 - 4\left[\frac{E(1, \nu_1, \nu_2 + 1, \nu_3, 1^e) - E(0, \nu_1, \nu_2, \nu_3, 0^e)}{E(0, \nu_1, \nu_2 + 2, \nu_3, 0^e) - E(0, \nu_1, \nu_2, \nu_3, 0^e)}\right]. \tag{24}$$

The parameter equals -1 for an ideal linear molecule and $+1$ for an ideal bent molecule. Bunker and Howe (*29*) generalized this definition to

$$\gamma^{BH}_{\nu_1\nu_2\nu_3} = 1 - 4\left[\frac{E(1, \nu_1, \nu_2 + 1, \nu_3, 1^e) + E(1, \nu_1, \nu_2, \nu_3, 0^e) - 2E(0, \nu_1, \nu_2, \nu_3, 0^e)}{E(0, \nu_1, \nu_2 + 2, \nu_3, 0^e) - E(0, \nu_1, \nu_2, \nu_3, 0^e)}\right] \tag{25}$$

which has the additional limit of -3 for an ideal free rotor. We note that as the rotational transition included in γ^{BH} will always be positive, $\gamma^{YW}_{\nu_1\nu_2\nu_3} > \gamma^{BH}_{\nu_1\nu_2\nu_3}$.

In Table VII we present correlation parameters for the vibrational states where all the necessary designations are possible. Both parameters give similar results: that the ground state is far from an ideal bent molecule and there is a further shift towards "quasi-linearity" with vibrational excitation. There is no evidence from γ^{BH} for free-rotor-like states ($\gamma^{BH} < -1$); however, work on LiCN (*10*) has shown that for real

TABLE VII

Yamada–Winnewisser (*28*) and Bunker–Howe (*29*) Correlation Parameters for the Low-Lying Vibrational States of CH_2^+ (see text for details)

v_1	v_2	v_3	$\gamma^{YW}_{v_1v_2v_3}$	$\gamma^{BH}_{v_1v_2v_3}$
0	0	0	0.34	0.26
0	2	0	-0.51	-0.58
0	4	0	-0.82	-0.87
0	6	0	-0.51	-0.57
1	0	0	-0.47	-0.52
0	8	0	-0.54	-0.60
0	0	1	0.32	0.23
0	2	1	-0.53	-0.61

(i.e., multidimensional) vibrational states that correlate with the free rotor limit, it is very difficult to label the various vibrational modes.

5. CONCLUSION

We have successfully obtained the low lying vibrational states of CH_2^+ using a method based on body-fixed atom–diatom collision coordinates. This has enabled us to obtain not only the fundamental vibrational levels, which are in good agreement with results (*2*) previously obtained using Watson's Hamiltonian for linear molecules (*6*), but also several combinations and overtones. The satisfactory convergence properties of this adapted method suggest that it could be applied to any floppy triatomic with confidence and it has been implemented as fully documented programs (*13, 30*).

Calculations on the $J = 1$ state show that CH_2^+ cannot easily be classified according to any ideal structure (linear, bent, or free rotor). This suggests that any basis set constructed as a displacement from some equilibrium structure will always give poor convergence.

Embedding along the R axis leads to unusually large off-diagonal Coriolis interactions and neglect of them makes the results qualitatively incorrect. On the other hand embedding along the r axis leads to relatively small off-diagonal Coriolis interactions and neglect of these still allows qualitatively correct results to be obtained, though the quantitative errors are still quite large compared to these observed in some previous calculations (*10, 11, 21*).

ACKNOWLEDGMENT

Thanks are due to Dr. Stuart Carter for helpful discussions about the results of his calculations.

RECEIVED: March 21, 1983

Note added in proof. Preliminary results of this work were used by Carter *et al.* (S. Carter, N. C. Handy, and B. T. Sutcliffe, *Mol. Phys.* **49,** 745–748 (1983) for testing a bond length–bond angle formalism for this problem. While their results generally confirm those of this work, several of the $J = 1$ results exhibit a measure of disagreement. The levels involved correspond to the ones perturbed most strongly by Coriolis interactions due to near degeneracies.

REFERENCES

1. R. Bartholomae, D. Martin, and B. T. Sutcliffe, *J. Mol. Spectrosc.* **87,** 367–381 (1981).
2. S. Carter and N. C. Handy, *J. Mol. Spectrosc.* **95,** 9–19 (1982).
3. R. J. Whitehead and N. C. Handy, *J. Mol. Spectrosc.* **55,** 356–373 (1975).
4. C. Eckart, *Phys. Rev.* **47,** 552–558 (1935).
5. J. K. G. Watson, *Mol. Phys.* **15,** 479–490 (1968).
6. J. K. G. Watson, *Mol. Phys.* **19,** 465–488 (1970).
7. B. T. Sutcliffe, *Mol. Phys.* **48,** 561–566 (1983).
8. S. Carter and N. C. Handy, *Mol. Phys.* **47,** 1445–1456 (1982).
9. J. Tennyson and A. van der Avoird, *J. Chem. Phys.* **76,** 5710–5718.
10. G. H. L. A. Brocks and J. Tennyson, *J. Mol. Spectrosc.* **99,** 263–278 (1983).
11. J. Tennyson and B. T. Sutcliffe, *J. Chem. Phys.* **77,** 4061–4072 (1982).
12. J. Tennyson and B. T. Sutcliffe, *J. Chem. Phys.* **79,** 43–51 (1983).
13. J. Tennyson, program ATOMDIAT, *Comput. Phys. Commun.* **29,** 307–319 (1983).
14. K. S. Sorbie and J. N. Murrell, *Mol. Phys.* **29,** 1387–1407 (1975).
15. V. A. Istomin, N. F. Stepanov, and B. I. Zhilinskii, *J. Mol. Spectrosc.* **67,** 265–282 (1977).
16. E. U. Condon and G. H. Shortley, "The Theory of Atomic Spectra," Cambridge Univ. Press, Cambridge, 1935.
17. D. M. Brink and G. R. Satchler, "Angular Momentum," 2nd Ed., Clarendon, Oxford, 1968.
18. J. M. Brown, T. J. Hougen, K.-P. Huber, J. W. C. Johns, I. Kopp, H. Lefrebvre-Brion, A. J. Merer, D. A. Ramsay, J. Rostos, and R. N. Zare, *J. Mol. Spectrosc.* **55,** 500–503 (1975).
19. A. M. Arthurs and A. Dalgarno, *Proc. R. Soc. London Ser. A* **256,** 540–551 (1960).
20. R. J. LeRoy and J. van Kranendonk, *J. Chem. Phys.* **61,** 4750–4769 (1974).
21. J. Tennyson and A. van der Avoird, *J. Chem. Phys.* **77,** 5664–5681 (1982).
22. I. S. Gradshteyn and I. H. Ryzhik, "Tables of Integrals, Series and Products," Academic Press, New York, 1980.
23. E. M. Greenwalt and A. S. Dickinson, *J. Mol. Spectrosc.* **30,** 427–436 (1969).
24. A. H. Stroud and D. Secrest, "Gaussian Quadrature Formulas," Prentice-Hall, London, 1946.
25. D. ter Haar, *Phys. Rev.* **70,** 222–223 (1946).
26. G. Herzberg, "Molecular Spectra and Molecular Structure, Vol. 2: Infrared and Raman Spectra of Polyatomic Molecules," Van Nostrand, New York, 1945.
27. T. J. Sears, P. R. Bunker, and A. R. W. McKellar, *J. Chem. Phys.* **77,** 5363–5369 (1982).
28. K. Yamada and M. Winnewisser, *Z. Naturforsch. A* **31,** 139–144 (1976).
29. P. R. Bunker and D. J. Howe, *J. Mol. Spectrosc.* **83,** 288–303 (1980).
30. J. Tennyson, programs ATOMDIAT2 and GENPOT, *Comput. Phys. Commun.*, in press.